International Information and Engineering Technology Association
Advancing the World of Information and Engineering

Ingénierie des Systèmes d'Information
Vol. 29, No. 4, August, 2024, pp. 1483-1491
Journal homepage: http://iieta.org/journals/isi

Enhancing Color Selection in HSV Color Space

Toni Kusnandar[1,2*], Judhi Santoso[1], Kridanto Surendro[1]

[1] School of Electrical Engineering and Informatic, Institut Teknologi Bandung, Bandung 40116, Indonesia
[2] Informatics Engineering, STMIK Mardira Indonesia, Bandung 40235, Indonesia

Corresponding Author Email: tonikusnandar@stmik-mi.ac.id

https://doi.org/10.18280/isi.290421

Received: 7 November 2023
Revised: 9 April 2024
Accepted: 30 May 2024
Available online: 21 August 2024

Keywords:
color constancy, color selection, heavy sidestep function, HSV color space

ABSTRACT

Vegetation indices measure plant health by capturing the green light reflected by plants as well as the red and blue light absorbed by plants. In order to ensure that the information that was originally gathered from the real world is replicated without any of the information being changed, color space transformation is utilized. Transformations of color spaces often lose information, and mapping colors are no exception. Utilizing UAVs to process plant health data in vast agricultural fields is highly efficient but requires rapid computational processing and streamlined steps. Using the Heaviside step function to make it easier and faster to choose the colors you want in the HSV color space is what this study is mostly about. In order to make modifications, the green color that had a hue value that ranged from 90 to 150 degrees was separated. Based on the findings that were revised at the time, it was determined that green can be differentiated from other hues. A modification that was recommended was shown to boost the processing speed by an average of 46.00 seconds, as indicated by the results of the trials that were carried out on images that were taken by an unmanned aerial vehicle (UAV).

1. INTRODUCTION

The human visual system is comprised of three components that collaborate to provide the sensation of color in the human perception. For the purpose of generating the whole range of colors, color displays make use of this concept by blending the three primary hues. These three colors are the basis for every imaginable hue in digital displays [1]. In farming, color analysis methods should be able to handle difficult capture conditions like shadows, noise, pixel saturation, low lighting, different types of crops, and the cameras' own built-in features [2]. Grayscale and RGB are not the best color spaces (CS) for detecting foreground objects, especially on dynamic backgrounds. For background modeling, standards like YCbCr or HSV have been suggested in the literature. However, the best results have been found when using different CSs for each application, scene, algorithm, etc. [3].

The Heavy sidestep function (HSF), is a key idea in the academic fields of engineering mathematics and operational calculus. This is a piecewise-defined function that is utilized in a wide range of engineering procedures and computations involving engineering. Non-elementary special functions or infinitesimal quantities are not used in the function's representation, which is typically represented using algebraic expressions. It does not represent the end of a sequence of functions and can be more appropriate and useful in computational techniques. Logic gates, neural networks, and optimization problems all use the function. It is analytically expressible and is frequently used in simulations and mathematical modeling [4-6].

There are numerous applications for the HSF in various fields. It serves as the foundation for the Turing Machine and logic circuits in computation and machine intelligence [5]. The HSF is utilized in operational calculus and engineering mathematics for computational procedures and techniques [7]. Robotics uses the HSF in nonlinear hierarchical least-squares programming for time-optimal control of nonlinear dynamic systems [8]. In finite-difference simulations, the HSF is used to make sharp internal boundaries with high spatial accuracy [9].

The HSF has been applied in various image processing applications. One method involves binary classification of image components as "smooth" and "non-smooth" using approximated Heaviside functions (AHFs) [5]. Another method adds to the binary classification different levels of smoothness and non-smoothness, showing parts with different AHF classes [10]. This method also incorporates l1 regularization for the coefficients of the non-smooth components and uses iterative refinement to capture more image details [11].

Color selection in agriculture faces several challenges. One challenge is dealing with non-trivial capture conditions such as shadows, noise, pixel saturation, low lighting, different crop varieties, and camera parameters [2]. Another challenge is selecting the optimal CS for each application domain. Previous studies have shown the importance of choosing the right CS for accurate color analysis in agriculture [12]. Additionally, there is a need for accurate and efficient color analysis techniques that can handle these challenges [12].

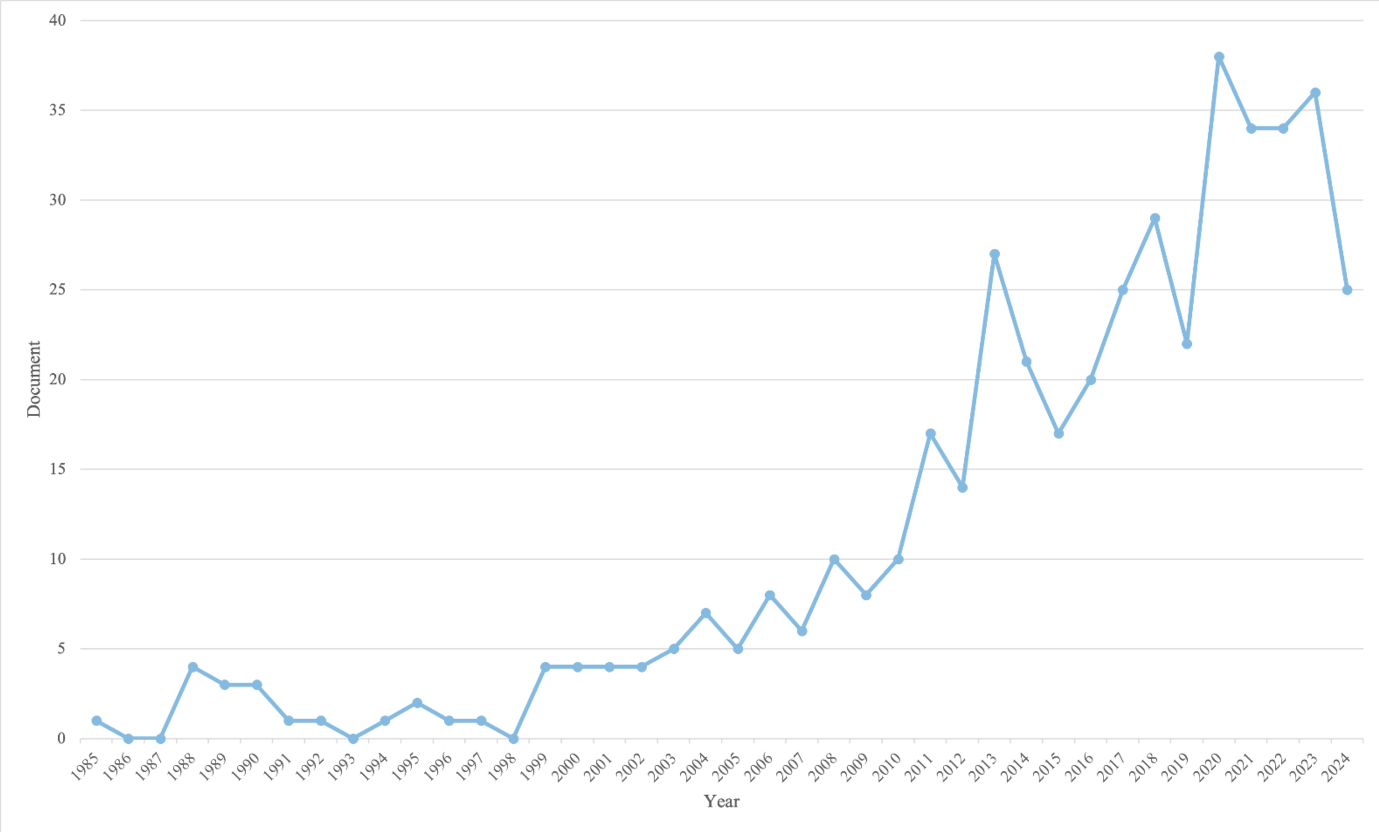

Figure 1. Related research color selection using HSV CS

Related study color selection using HSV CS is still regularly found (833 documents), with a trend that can be shown in Figure 1 showing that 833 papers were located using the string "(TITLE-ABS-KEY (color AND selection) AND ((HSV OR hue OR saturation) OR (color AND space))) AND (LIMIT-TO (SUBJAREA, "COMP")) AND (LIMIT-TO (DOCTYPE, "ar") OR LIMIT-TO (DOCTYPE, "re")) AND (LIMIT-TO (PUBSTAGE, "final")) AND (LIMIT-TO (SRCTYPE, "j")) AND (LIMIT-TO (LANGUAGE, "English"))" to search the Scopus database. This shows that studies on HSV or CS color filtering are still being conducted.

The advantages of using the HSV CS for color selection include its ability to reduce the color spectrum and select candidates for specific skin tones [13]. It also allows for the categorization of colors in images, making it useful for object categorization and detection [14]. Additionally, the HSV CS can be utilized to estimate the amount of airlight in hazy images, improving the quality of dehazed images [15]. On the other hand, the disadvantages of using the HSV CS for color selection include the fogginess that can occur when applying color classification due to the gradient between each color [16]. Furthermore, while the HSV CS-based retrieval system shows higher retrieval accuracy compared to other CSs, it may still have limitations in terms of precision, recall, and response time [17].

2. RELATED WORKS

Plant color selection in the HSV CS has been investigated in several papers. Gunal et al. (2008) found that using HSV color components for image segmentation provided results as good as using gray scale values only [18]. Chen et al. proposed an algorithm that utilizes the HSV CS for processing chili pepper images, which resulted in superior precision and recall compared to the RGB CS [19]. Wang and Zhao analyzed the denoising processing of color forest dynamic inspection images and concluded that applying HSI or YCbCr CS is advantageous in terms of faster execution and better fit for less noise, while applying RGB CS is advantageous for more noise [20]. Lu et al. [21] discussed a color matching method for colored fiber blends using the fuzzy C-mean cluster approach in the HSV CS.

Schwarz et al. [22] conducted color matching experiments on five color models: RGB, Opponent, YIQ, LAB, and HSV. They compared the selection speed and precision of colors. The experiment revealed that the RGB color model resulted in the quickest color selection time but the lowest accuracy, while the HSV color model resulted in the slowest color selection time but the highest accuracy. They also discovered that user learning occurs with the Opponent, YIQ, LAB, and HSV color models, but not with the RGB color model. Research conducted by Garcia et al. [23] mentioned, Fruit recognition in supermarkets that uses computer vision focuses on color chromaticity, which is a key part of figuring out the shape and texture of fruits. The HSV space is proposed for color extraction because it lets processing happen without the effects of intensity that come with the RGB space.

The color sequence system makes it possible to describe color stimuli with certainty. Ones that are used are RGB, CMYK, and CIELAB. Brightness, chroma, and hue circles are shown as angles in Figure 2, which is a three-dimensional shape of a color system. In terms of luminance and chroma, this makes a pretty uniform color scale. It also makes a scale that is similar along the hue circle [24]. Digital images are typically provided by imaging devices as RGB data, which uses a standard CS to represent the image. Because it contains red, green, and blue, RGB is often referred to as the "primary colors of light" [25].

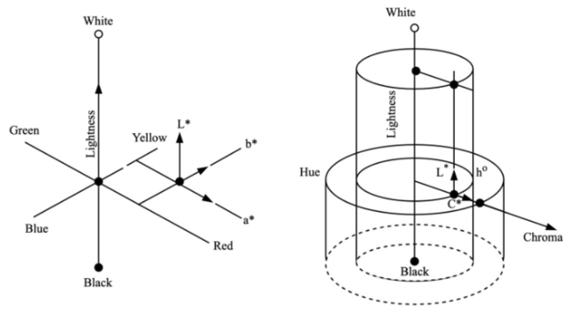

Figure 2. Three-dimensional graphics that depict the colors of the actual surface, with chroma, hue, and brightness systems are included [24]

It is necessary for an HSV fruit recognition method that makes use of color chromaticity to extract and evaluate chromaticity data without the influence of an RGB space on the intensity of the measurements [23]. Through the use of an HSV color segmentation algorithm that automatically determines the optimal saturation channel threshold value, the leaves are separated the ill areas on the leaves are spread out, and they are visible from the background [26]. To avoid color shifts and simplify processing, haze is also removed using the HSV CS [27]. Hue is preserved through the use of perceptual color models like HSI and HSV. There is a suggestion for a saturation correction algorithm. The processing result in an ideal HSI CS with the same RGB gamut matches the adjusted saturation value. Because standard RGB CS transition typically produces gamut issues [28].

There are several other methods for color selection besides HSV CS. One approach is the YCbCr CS, which has been found to be efficient for the segmentation and detection of skin color in color images [29]. Another method is the vector ordering based on the combination of hue (H), saturation (S), and value (V), which has been shown to effectively reduce color noise in color image processing [30]. Additionally, there are schemes for spectral sampling and computation that can be used to select a color computation space based on relevant considerations [31]. In the context of texture classification, a multi-CS histogram selection (MCSHS) approach has been proposed, which combines multiple CSs to achieve good performances in accuracy and computation time [32]. Finally, the HSV CS has been suggested as a useful tool for vehicle detection at nighttime, as it allows for the extraction of license plates by highlighting the headlights or taillights of vehicles [33].

Transforming to a different CS is necessary because Non-uniform RGB has restrictions and biases toward differing color intensities. A perceptual translation from an additive RGB model to a single CS standardizes everything. Normalizing the r, g, and b values of each pixel in an image is the first step in the RGB to HSV conversion process [34]:

$$r = \frac{R}{R+G+B} \tag{1}$$

$$g = \frac{G}{R+G+B} \tag{2}$$

$$b = \frac{B}{R+G+B} \tag{3}$$

The following equation is used to perform the transformation from RGB to HSV after the RGB normalization has been completed:

$$V = max(r, g, b) \tag{4}$$

$$S = \begin{cases} 0 & if\ V = 0 \\ V - \dfrac{min(r,g,b)}{V} & if\ V > 0 \end{cases} \tag{5}$$

$$H = \begin{cases} 0 & if\ S = 0 \\ 60^o \times \left[\dfrac{g-b}{S \times V}\right] & if\ V = r \\ 60^o \times \left[2 + \dfrac{b-r}{S \times V}\right] & if\ max = g \\ 60^o \times \left[4 + \dfrac{r-g}{S \times V}\right] & if\ max = b \\ H + 360^o & if\ H < 0 \end{cases} \tag{6}$$

The equation for transforming RGB to HSV is a function that is characterized by being piecewise constant. This function can be expressed using the HSF or Unit Step Function [35, 36]. When the constants in localized parts of a function are separated by an unlimited number of conceivable boundaries of smaller dimensions, the function is said to be piecewise constant [36].

3. PROPOSED METHOD

Photosynthesis requires chlorophyll pigment a and b to selectively capture blue (400-500nm) and red (600-700nm) light. The absorption of green wavelengths (500-600 nm) is still minimal, which means that the green color is a distinctive feature of thriving vegetation [37, 38]. There is a strong affinity for absorption within the blue wavelength region (400-500nm) for the pigment known as carotene, which can range from yellow to orange-red in nature. Similarly, red and blue pigments also exhibit significant absorption within the 400-500nm range, thereby influencing the diverse array of hues observed in autumn foliage [37].

It is the light waves that are reflected from things that provide the visual system of humans with its color information. The wavelength of the light and the reflectance properties of the objects that these light waves reflect both have an effect on the light waves that are being communicated [39]. In the investigation regarding methodologies for achieving perfect reflectance, it was discovered that objects which possess a proficient ability to reflect light are capable of generating valuable reflectance data [40]. The magnitude of luminosity reflection or luminosity intensity in digital images may be acquired from various CSs that serve as mathematical depictions of a collection of hues [41].

The loss of information is common when transforming between CS, examples include translating across color gamuts, transforming multiprimary or multispectral data into tristimulus space, and mapping colors to grayscale [42]. Image processing is a basic component, and the transformation of CS is a crucial feature of real-world observation that is made possible by camera equipment to enable [43, 44]. Achieving a faithful reproduction of real-world data without changing any facts is the goal of CS transformation. To replicate the genuineness of tangible images and acquire the essential data aligned with their designated purposes, diverse CS models are employed. Consequently, the requirement for CS transformation assumes a significant role [43].

For the purpose of modifying the color sorting for plant photographs, it was suggested that the green color that is reflected by vegetation through the process of photosynthetic separation be separated. This was based on the justifications that were presented [37, 38, 41, 43]. This suggested alteration involves the arrangement of the green hue that is emitted by plants while undergoing the process of photosynthesis. By utilizing HSV CS, a channel that has color was isolated from the level of intensity and the saturation channels, resulting in more accurate processed plant photos. Images that were taken with a camera that worked with visible light were converted into RGB images with flaws [34], thus HSV CS transformation is needed [43]. The suggested modification of the CS transformation only picked the green color, precisely within the hue range of 90° to 150°. This was done in light of the fact that photosynthesis exhibits a significant degree of green color reflection [37, 38, 41]. The RGB visible light camera that was put on the unmanned aerial vehicle (UAV) to take pictures of plants was used. Images of plants were taken with an RGB visible light camera that was mounted on a UAV. This portion of the investigation began with the collecting of plant images. The RGB images were then transformed into the HSV CS. The conversion from RGB to HSV is performed due to the enhanced stability of color values in the HSV CS [45]. Using the first procedure, the conventional transformation was carried out, whereas in the second method, modified transformation was used.

According to the traditional way of transformation, each and every color was transformed into HSV images. Since plants' green tint indicates healthy photosynthesis [37, 38, 46, 47] the proposed method sorted greens with wavelength values ranging from 500nm to 600nm or hue values ranging from 90° to 150°. Filtering for hue values between 90 and 150 was added to the standard algorithm for transforming colors between the HSV space. Once the HSV images were obtained, the green color was separated out so that the final images contained only green. Meanwhile, color sorting was done during the transformation process in the revised transformation method. The proposed method produced HSV images where only green was prioritized. After that, we proceeded to assess the chosen green HSV images. Figure 3 depicts the entire procedure used in this investigation.

The segmentation of color channels within the HSV CS enables a more precise color selection procedure since it remains unaffected by intensity and saturation. The process of selecting the desired color will involve the examination of each color pixel within the Hue channel. When the pixels are selected, they will produce a value of '1' if the conditions are met and '0' if they are not. This selection scenario can be streamlined utilizing the HSF, which can verify the desired criteria and provide an output of '0' or '1' based on the specified condition.

This adjustment resulted in a more straightforward HSF-based CS transformation formula, as shown in Figure 4.

One possible representation of the formula that makes use of the HSF is as follows:

$$H = H^o\left(\mathcal{H}(H^o - 90^o) - \mathcal{H}(H^o - 150^o)\right) \tag{7}$$

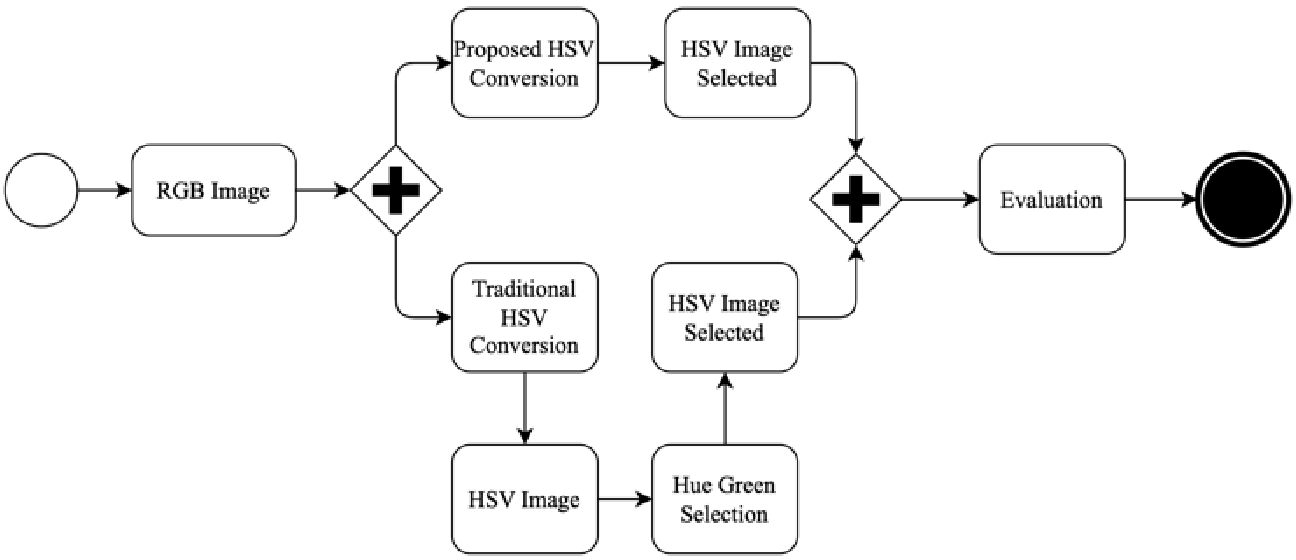

Figure 3. Research stages

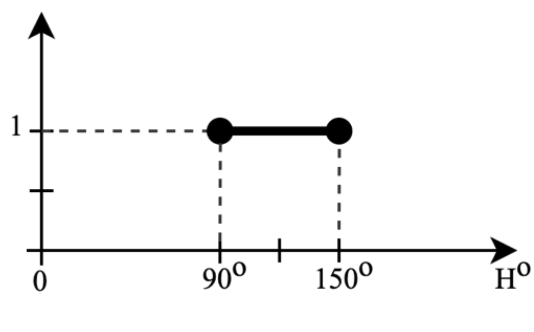

(a) $\mathrm{H} = \mathrm{H}^o\left(\mathcal{H}(\mathrm{H}^o - 90^o) - \mathcal{H}(\mathrm{H}^o - 150^o)\right)$

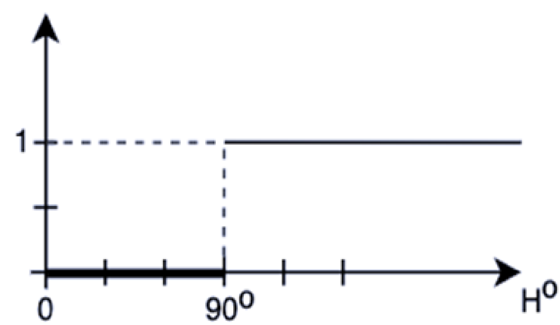

(b) $\mathcal{H}(H^o - 90^o)$

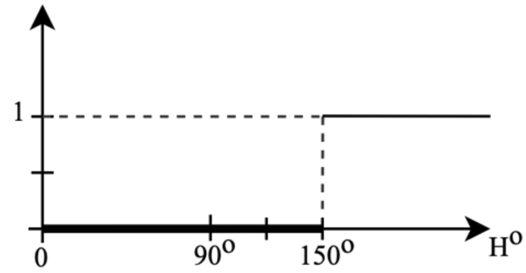

(c) $\mathcal{H}(\mathrm{H}^{o} - 150^{o})$

Figure 4. Formula enhancing color selection in HSV CS

4. EXPERIMENT RESULT

There were photographs of various kinds of plants, properties, structures, and other objects included in the data collection that was utilized. The selection of this dataset was made in order to evaluate the precision of the color selection technique that was suggested. Within each dataset, there is a range of objects displaying diverse colors, leading to the assessment of the efficacy of the proposed method in isolating the specific colors of interest. The dataset acquisition was carried out utilizing UAVs, with the anticipation that this approach could potentially be deployed in vast agricultural areas. Data was captured using a Phatom 3 Advance UAV quadcopter drone camera and translated into digital photos. The camera that was used has consistent characteristics across all of the datasets, including a focal length that is always 3.61 millimeters, a F number of f/2.8, and an RGB CS. Table 1 contains a comprehensive listing of the image dataset's features and specifications for your perusal [48].

The findings of this study were validated using five different datasets, and the total amount of time spent computing was tallied. In the experiment, a MacBook Air 2017 was utilized. An Intel Core i5 processor with two cores operating at 1.8GHz, eight gigabytes of DDR3 memory operating at 1600 MHz, and an Intel HD Graphics 6000 with 1536 megabytes of RAM were all included in this particular model. By converting from RGB to HSV, the experiment successfully isolated the green hue between 90 and 150 degrees. The computation time for this transformation was reduced by sorting the colors concurrently with the transformation. Time spent computing was cut by between 39,60 second and 53,62 second compared to the conventional approach (Table 2). This comparison is made by comparing the standard computation time to the computing time of the proposed method. The total computing values are added together, and the average speed difference is computed [48].

Table 1. Features of the dataset [48]

Dataset Characteristic	Dataset				
	North Konawe Oil Palm Plantation (NKOPP)	Ciwidey Cabbage Farm	FSRD ITB Bandung	North Gate ITB Bandung	Cipularang Highway KM 88
Dimension	4000x3000	4000x3000	4000x2250	4000x3000	4000x3000
Device model	DJI FC300S	DJI FC300S	DJI FC300S	DJI FC300S	DJI FC300S
Color space	RGB	RGB	RGB	RGB	RGB
Focal length	3,61 mm	3,61 mm	3,61 mm	3,61 mm	3,61 mm
F number	f/2,8	f/2,8	f/2,8	f/2,8	f/2,8
Exposure time	1/488	1/100	1/781	1/301	1/800
Exposure program	Normal	Normal	Normal	Normal	Manual
Latitude	3° 16' 46,686" S	7° 7' 50,14" S	6° 53' 33,21" S	6° 53' 16,11" S	6° 36' 10,284" S
Longitude	22° 15' 17,406" E	107° 24' 51,222" E	107° 36' 45,03" E	107° 36' 36,3" E	107° 25' 30,03" E

Table 2. Experiment results [48]

No	Dataset	Computing Time (In Second)		Speed Enhancement
		Traditional	Our Method	
1	NKOPP	268.275376	214.650387	53.62
2	Ciwidey Cabbage Farm	268.275376	223.447875	44.83
3	FSRD ITB Bandung	217.654637	172.204226	45.45
4	North Gate ITB	308.873992	262.398893	46.48
5	Cipularang Highway KM 88	279.611737	240.014733	39.60
				46.00

(a) Image before selection

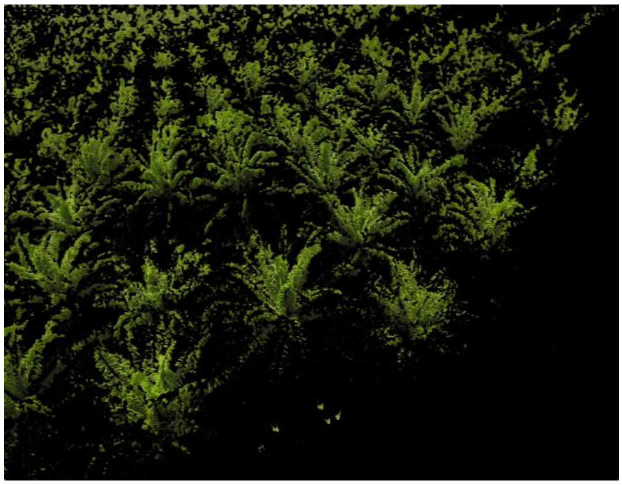

(b) Image after selection

Figure 5. Image of an NKOPP

The results of the experiments with the dataset comprising of images captured at the NKOPP are which are depicted in Figures 5 and 6, respectively. Figure 5 (a) and Figure 6 (a) are RGB photos; Figure 5 (b) and Figure 6 (b) are HSV CS images that have had the green color transformed and sorted; the target green color has been effectively isolated.

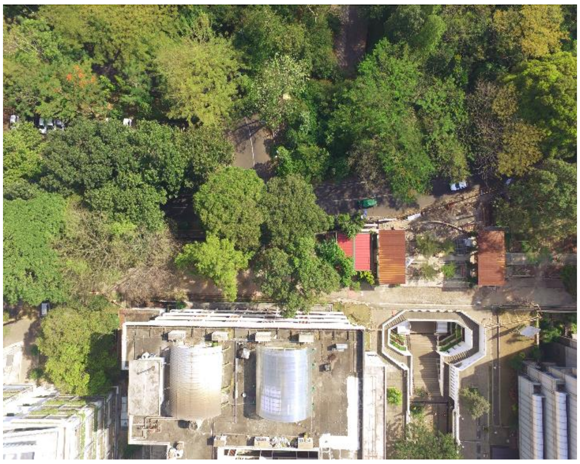

(a) Image before selection

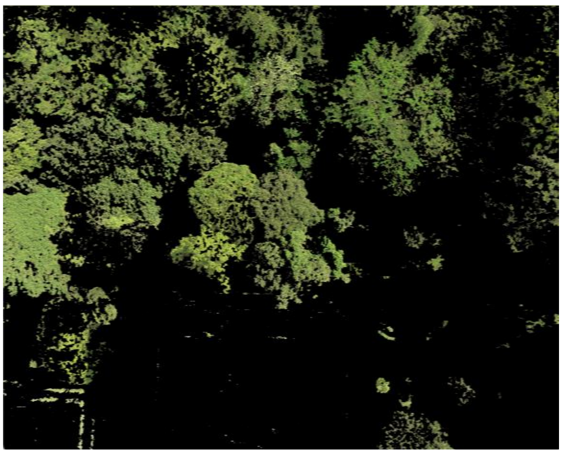

(b) Image after selection

Figure 6. Image of the North Entrance to ITB

5. DISCUSSION

Experiments have successfully streamlined the color selection procedure and accelerated computational processing speed. Upon closer inspection, it was discovered that there are still flaws, as other color areas were not meticulously chosen. Despite the fact that these are not the desired colors for selection, additional research or optimization is required to achieve perfect color selection. As shown in Figure 7, there are still color regions that cannot be selected flawlessly. The image on the left displays the result of selecting the green color from the image on the right. Even though the white color that appears is not the result of choosing the desired green color, it is necessary to investigate why this occurs.

Figure 7. Color selection still needs to be optimized

In addition to the problem of incorrect color selection, there is also a need for improvements in terms of how long computations take. If this color selection method is to be implemented on a UAV, then a faster processing time is required, which means that the computational time must be increased. When using a UAV to perform real-time color selection, it is absolutely necessary to have an extremely fast processing time.

The findings of this study call for a further increase in computing speed to less than 1 second in order to apply it to UAV cameras in real time. Once this goal has been met, it will be possible to identify agricultural regions and monitor plant health problems in real time.

6. CONCLUSION

With regard to this investigation, the solution that has been proposed is capable of modifying the sorting of the green color in a manner that is not only satisfactory but also results in a faster computation time of forty-six seconds. This is accomplished during the steps of conversion RGB images to HSV. The method that has been developed is able to differentiate between a wide range of colors in addition to green since it provides the appropriate range of hue values. Through the utilization of this method, the process of color sorting in HSV photos may be shortened, and the formula can be simplified through the utilization of the Heaviside Step Function.

The proposed method contributes by enabling novel possibilities for conducting color selection with reduced computational time. The expedited color selection procedure may be applied in precision agriculture (PA) operations utilizing unmanned aerial vehicles (UAVs) in a real-time fashion.

During the course of further research, it is suggested that an investigation be carried out into the idea that the values of the parameters in HSV imagery might be understood as a representation of the total amount of light. This has been suggested as a potential future research direction. It is envisaged that this will make it possible for it to ascertain the existence of a connection between the values of the parameters and the mechanism of photosynthesis that takes place in plants.

REFERENCES

[1] Ansari, M., Singh, D.K. (2022). Significance of color spaces and their selection for image processing: A survey. Recent Advances in Computer Science and Communications (Formerly: Recent Patents on Computer Science), 15(7): 946-956. https://doi.org/10.2174/2666255814666210308152108

[2] Hernández-Hernández, J.L., García-Mateos, G., González-Esquiva, J.M., Escarabajal-Henarejos, D., Ruiz-Canales, A., Molina-Martínez, J.M. (2016). Optimal color space selection method for plant/soil segmentation in agriculture. Computers and Electronics in Agriculture, 122: 124-132. https://doi.org/10.1016/j.compag.2016.01.020

[3] López-Rubio, F.J., Domínguez, E., Palomo, E.J., López-Rubio, E., Luque-Baena, R.M. (2016). Selecting the color space for self-organizing map based foreground detection in video. Neural Processing Letters, 43: 345-361. https://doi.org/10.1007/s11063-015-9431-8

[4] Hatano, N., Ikeda, M., Ishikawa, I., Sawano, Y. (2023). Heaviside function as an activation function. Journal of Applied Analysis, 29(1): 1-2. https://doi.org/10.1515/jaa-2022-2012

[5] Iacovelli, G., Iacovelli, C. (2022). Representing logic gates over Euclidean space via heaviside step function. Scientific Reports, 12(1): 8009. https://doi.org/10.1038/s41598-022-11941-y

[6] Venetis, J.C. (2023). An explicit expression of the unit step function. International Review of Electrical Engineering, 18(1): 83-87. https://doi.org/10.15866/iree.v18i1.23117

[7] Venetis, J. (2021). An explicit form of heaviside step function. Mathematics & Computer Science, Preprints, 2021: 2021060132. https://doi.org/10.20944/preprints202106.0132.v1

[8] Pfeiffer, K., Pham, Q.C. (2023). Time-Optimal control via heaviside step-function approximation. In 2023 IEEE/RSJ International Conference on Intelligent Robots and Systems (IROS), Detroit, MI, USA, pp. 8223-8230. https://doi.org/10.48550/ARXIV.2303.04516

[9] Mittet, R. (2018). Implementing internal interfaces in finite-difference schemes with the Heaviside step function. In SEG International Exposition and Annual Meeting, Anaheim, California, USA, pp. SEG-2018. https://doi.org/10.1190/segam2018-2994775.1

[10] Legua, M.P., Morales, I., Sánchez Ruiz, L.M. (2008). The heaviside step function and MATLAB. In Computational Science and Its Applications-ICCSA 2008: International Conference, Perugia, Italy, Proceedings, Part I, 8, pp. 1212-1221. https://doi.org/10.1007/978-3-540-69839-5_93

[11] Haarsa, P., Pothat, S. (2015). The power series expansion on a bulge heaviside step function. Applied Mathematical Sciences, 9(23): 1125-1129.

[12] Wang, J., Zhou, Z., Huo, X., Dan, J., Kou, L. (2010). Information, credit reputation and the motivation of producing green agricultural products. In 2010 International Conference on Management and Service Science, Wuhan, China, pp. 1-4. https://doi.org/10.1109/ICMSS.2010.5576832

[13] Feitosa, R.D.F., da Silva Soares, A., Pereyra, L.C. (2018). A new clustering-based thresholding method for human skin segmentation using HSV color space. In 2018 IEEE Symposium on Computers and Communications (ISCC), Natal, Brazil, pp. 01177-01180. https://doi.org/10.1109/ISCC.2018.8538604

[14] Al-Hetar, A.M., Rassam, M.A., Shormani, O., Salem, A.S., Al-Yousofi, H. (2019). Color-based object categorization model using fuzzy HSV inference system. In 2019 First International Conference of Intelligent Computing and Engineering (ICOICE), Hadhramout, Yemen, pp. 1-6. https://doi.org/10.1109/ICOICE48418.2019.9035173

[15] Othman, M.K., Abdulla, A.A. (2022). Enhanced single image dehazing technique based on HSV color space. UHD Journal of Science and Technology, 6(2): 135-146. https://doi.org/10.21928/uhdjst.v6n2y2022.pp135-146

[16] Pavithra, L.K., Sree Sharmila, T. (2017). Retrieval of homogeneous images using appropriate color space selection. In Computational Intelligence in Data Mining: Proceedings of the International Conference on CIDM, 10-11 December 2016. Springer, Singapore, pp. 739-747. https://doi.org/10.1007/978-981-10-3874-7_70

[17] Xia, Y., Wang, S., Li, Y., You, L., Yang, X., Zhang, J.J. (2020). Single color sketch-based image retrieval in HSV color space. Transactions on Computational Science XXXVII: Special Issue on Computer Graphics, Springer, Berlin, Heidelberg, 77-90. https://doi.org/10.1007/978-3-662-61983-4_5

[18] Gunal, E.S., Canbek, S., Adar, N., Goktogan, A.H. (2008). Plant classification using fractal dimension in HSV color space. In 2008 IEEE 16th Signal Processing, Communication and Applications Conference, Aydin, Turkey, pp. 1-4. http://dx.doi.org/10.1109/SIU.2008.4632696

[19] Chen, W., Gao, H., Ding, D., Dong, X., Luo, X. (2023). Chili pepper pests recognition based on HSV color space and convolutional neural networks. In 2023 IEEE 3rd International Conference on Electronic Technology,

Communication and Information (ICETCI), Changchun, China, pp. 241-245. https://doi.org/10.1109/ICETCI57876.2023.10176415

[20] Wang, J., Zhao, W. (2010). A method of color space selection for color forest inspection image denoising applications. In 2010 3rd International Conference on Advanced Computer Theory and Engineering (ICACTE), Chengdu, 4: V4-207. https://doi.org/10.1109/ICACTE.2010.5579712

[21] Lu, Y., Gao, W., Liu, J. (2010). Color matching for colored fiber blends based on the fuzzy c-mean cluster in HSV color space. In 2010 Seventh International Conference on Fuzzy Systems and Knowledge Discovery, Yantai, China, 1: 452-455. https://doi.org/10.1109/FSKD.2010.5569615

[22] Schwarz, M.W., Cowan, W.B., Beatty, J.C. (1987). An experimental comparison of RGB, YIQ, LAB, HSV, and opponent color models. ACM Transactions on Graphics (tog), 6(2): 123-158. https://doi.org/10.1145/31336.31338

[23] Garcia, F., Cervantes, J., López, A., Alvarado, M. (2016). Fruit classification by extracting color chromaticity, shape and texture features: Towards an application for supermarkets. IEEE Latin America Transactions, 14(7): 3434-3443. https://doi.org/10.1109/TLA.2016.7587652

[24] Best, J. (Ed.). (2017). Colour design: Theories and applications. Second Edition. In The Textile Institute book series. Cambridge, MA: Elsevier.

[25] Kumar, A., Malhotra, S. (2015). Performance analysis of color space for optimum skin color detection. In 2015 Fifth International Conference on Communication Systems and Network Technologies, Gwalior, India, pp. 554-558. https://doi.org/10.1109/CSNT.2015.88

[26] Waldamichael, F.G., Debelee, T.G., Ayano, Y.M. (2022). Coffee disease detection using a robust HSV color-based segmentation and transfer learning for use on smartphones. International Journal of Intelligent Systems, 37(8): 4967-4993. http://doi.org/10.1002/int.22747

[27] Zhang, T., Hu, H.M., Li, B. (2018). A naturalness preserved fast dehazing algorithm using HSV color space. IEEE Access, 6: 10644-10649. https://doi.org/10.1109/ACCESS.2018.2806372

[28] Kamiyama, M., Taguchi, A. (2021). Color conversion formula with saturation correction from HSI color space to RGB color space. IEICE Transactions on Fundamentals of Electronics, Communications and Computer Sciences, 104(7): 1000-1005. https://doi.org/10.1587/transfun.2020EAL2087

[29] Shaik, K.B., Ganesan, P., Kalist, V., Sathish, B.S., Jenitha, J.M.M. (2015). Comparative study of skin color detection and segmentation in HSV and YCbCr color space. Procedia Computer Science, 57: 41-48. https://doi.org/10.1016/j.procs.2015.07.362

[30] Lei, T., Wang, Y., Fan, Y., Zhao, J. (2013). Vector morphological operators in HSV color space. Science China Information Sciences, 56: 1-12. https://doi.org/10.1007/s11432-011-4475-5

[31] Hall, R. (1999). Comparing spectral color computation methods. IEEE Computer Graphics and Applications, 19(4): 36-45. https://doi.org/10.1109/38.773962

[32] Porebski, A., Vandenbroucke, N., Macaire, L. (2010). Comparison of feature selection schemes for color texture classification. In 2010 2nd International Conference on Image Processing Theory, Tools and Applications, Paris, France, pp. 32-37. https://doi.org/10.1109/IPTA.2010.5586760

[33] Park, H.S. (2015). Vehicle tracking system using HSV color space at nighttime. The Journal of Korea Institute of Information, Electronics, and Communication Technology, 8(4): 270-274. https://doi.org/10.17661/JKIIECT.2015.8.4.270

[34] Yu, L.S., Chou, S.Y., Wu, H.Y., Chen, Y.C., Chen, Y.H. (2021). Rapid and semi-quantitative colorimetric loop-mediated isothermal amplification detection of ASFV via HSV color model transformation. Journal of Microbiology, Immunology and Infection, 54(5): 963-970. https://doi.org/10.1016/j.jmii.2020.08.003

[35] Abramowitz, M., Stegun, I.A. (1972). Handbook of mathematical functions: With formulas, graphs and mathematical tables. In Conference under the Auspices of the National Science Foundation and the Massachussetts Institute of Technology, Unabridged, Unaltered and Corr. Republ. of the 1964 ed. in Dover Books on Advanced Mathematics. New York: Dover publ. https://personal.math.ubc.ca/~cbm/aands/abramowitz_and_stegun.pdf.

[36] Weisstein, E.W. (2002). Heaviside step function. MathWorld-A Wolfram Web Resource. https://mathworld.wolfram.com/HeavisideStepFunction.html.

[37] Huete, A.R. (2004). Remote sensing for environmental monitoring. Environmental Monitoring and Characterization, 183-206. https://doi.org/10.1016/B978-012064477-3/50013-8

[38] Smith, H.L., McAusland, L., Murchie, E.H. (2017). Don't ignore the green light: Exploring diverse roles in plant processes. Journal of Experimental Botany, 68(9): 2099-2110. https://doi.org/10.1093/jxb/erx098

[39] Gijsenij, A., Gevers, T., Van De Weijer, J. (2011). Computational color constancy: Survey and experiments. IEEE Transactions on Image Processing, 20(9): 2475-2489. https://doi.org/10.1109/TIP.2011.2118224

[40] Marlow, P.J., Kim, J., Anderson, B.L. (2012). The perception and misperception of specular surface reflectance. Current Biology, 22(20): 1909-1913. https://doi.org/10.1016/j.cub.2012.08.009

[41] Jack, K. (2007). Chapter 3-Color spaces. Video Demystified (Fifth Edition), pp. 15-36. https://doi.org/10.1016/B978-075068395-1/50003-1

[42] Lau, C., Heidrich, W., Mantiuk, R. (2011). Cluster-based color space optimizations. In 2011 International Conference on Computer Vision, Barcelona, Spain, pp. 1172-1179. https://doi.org/10.1109/ICCV.2011.6126366

[43] Jayashree, R.A. (2013). RGB to HSI color space conversion via MACT algorithm. In 2013 International Conference on Communication and Signal Processing, Melmaruvathur, India, pp. 561-565. https://doi.org/10.1109/iccsp.2013.6577117

[44] Zhang, Q., Kamata, S.I. (2016). A novel color space based on RGB color barycenter. In 2016 IEEE International Conference on Acoustics, Speech and Signal Processing (ICASSP), Shanghai, China, pp. 1601-1605. https://doi.org/10.1109/ICASSP.2016.7471947

[45] Kusnandar, T., Santoso, J., Surendro, K. (2023). A novel method for optimizing color selection using the hadamard product technique. IEEE Access, 11: 130155-130164.

https://doi.org/10.1109/ACCESS.2023.3333367
[46] Grant, R.H. (1997). Partitioning of biologically active radiation in plant canopies. International Journal of Biometeorology, 40: 26-40. https://doi.org/10.1007/BF02439408
[47] Kusnandar, T., Santoso, J., Surendro, K. (2023). The effect of white balance for color constancy on visible light. In Proceedings of the 2023 12th International Conference on Software and Computer Applications, New York, United States, pp. 144-149. https://doi.org/10.1145/3587828.3587850
[48] Kusnandar, T., Santoso, J., Surendro, K. (2023). Modification color filtering in HSV color space. Review, preprint. https://doi.org/10.21203/rs.3.rs-2650337/v1